Geophysical Prospecting, 2006, **54**, 565–573

Influence of pore pressure on velocity in low-porosity sandstone: Implications for time-lapse feasibility and pore-pressure study

Xiaoxia Xu,* Ronny Hofmann, Michael Batzle and Tashi Tshering
Colorado School of Mines, Department of Geophysics, Golden, CO 80401, USA

Received July 2005, revision accepted February 2006

ABSTRACT

As seismic data quality improves, time-lapse seismic data is increasingly being called upon to interpret and predict changes during reservoir development and production. Since pressure change is a major component of reservoir change during production, a thorough understanding of the influence of pore pressure on seismic velocity is critical. Laboratory measurements show that differential pressure (overburden minus fluid pressure) does not adequately determine the actual reservoir conditions. Changes in fluid pressure are found to have an additional effect on the physical properties of rocks. The effective-stress coefficient n is used to quantify the effect of pore pressure compared to confining pressure on rock properties. However, the current practice in time-lapse feasibility studies, reservoir-pressure inversion and pore-pressure prediction is to assume that $n = 1$. Laboratory measurements, reported in both this and previous research show that n can be significantly less than unity for low-porosity rocks and that it varies with porosity, rock texture and wave type.

We report the results of ultrasonic experiments to estimate n for low-porosity sandstones with and without microcracks. Our results show that, for P-waves, n is as low as 0.4 at a differential pressure of 20 MPa (about 3000 psi) for a low-porosity sandstone. Thus, in pore-pressure inversion, an assumption of $n = 1$ would lead to a 150% underestimation of the pore pressure. Comparison of the effective-stress coefficient for fractured and unfractured samples suggests that the presence of microfractures increases the sensitivity of P-wave velocity to pore pressure, and therefore the effective-stress coefficient. Our results show that the effective-stress coefficient decreases with the differential pressure, with a higher differential pressure resulting in a lower effective-stress coefficient. While the effective-stress coefficient for P-wave velocity can be significantly less than unity, it is close to one for S-waves.

INTRODUCTION

Pressure strongly influences the mechanical and transport properties of rocks, such as porosity, velocity, permeability and resistivity. In a fluid-saturated rock, both pore pressure and confining pressure control the rock properties. Seismic and borehole techniques measure these rock properties in order to infer subsurface information. For example, time-lapse seismic is often employed to find bypassed reserves and reservoir-pressure distribution. Differences in seismic attributes (a combination of compressional- and shear-wave velocities and density) between monitor and base surveys are used to infer pore pressure and saturation changes caused by depletion and injection.

To relate changes in seismic attributes to reservoir conditions, a thorough understanding of pressure and saturation effects on rock properties is essential. Gassmann's theory (1951) is generally accepted as a prediction tool for velocity change

*E-mail: xiaoxia@dix.mines.edu

with changing fluid type. As to the relationship between velocity and pressure, it is commonly assumed that differential pressure P_d is the governing factor (Landrø *et al*. 2003), given by

$$P_d = P_c - P_p, \tag{1}$$

where P_c is the confining pressure and P_p is the pore or reservoir pressure. This assumption implies that the influence of changes in P_c on the rock frame can be exactly offset by equal changes in P_p. Although the assumption works well in shallow reservoirs with unconsolidated rocks typical of the shallow Gulf of Mexico, it has been found inadequate for deep consolidated reservoirs. Hall *et al*. (2003) reported that the observed 4D signal (reflection amplitude) is much weaker than predicted in a Permian tight gas–sand reservoir in the North Sea. MacBeth *et al*. (2006) suggested that this discrepancy between prediction and observation might result from the assumption of a universal validity of equation (1).

Both rock-physics theory and experiments suggest that equation (1) is only an approximation that is valid for some lithologies. Although porosity has a direct influence on the effective-stress coefficient, it is not the only parameter that governs this coefficient. Measurements suggest that the effective-stress coefficient also depends on rock texture, rock type, wave mode and pressure regimes. From a practical standpoint, we need to know how the effective-stress coefficient changes with conditions and rock characteristics, so that, for a specific reservoir rock, the effective-stress coefficient can be estimated with reasonable certainty.

Previous research into effective stress has revealed some aspects of how the coefficient changes with differential pressure and with the microstructure of a rock. Todd and Simmons (1972) and Christensen and Wang (1985) observed that the effective-stress coefficient for compressional waves is approximately linearly dependent on the differential pressure. Comparing the effective-stress coefficients for Berea and Michigan sandstones, Prasad and Manghnani (1997) suggested that the presence of microcracks increases the sensitivity of the rock properties to pore pressure.

STRESS DEFINITIONS

Laboratory measurements have long suggested that the commonly used definition in equation (1) is an oversimplification of the actual stress state in a rock. A more accurate stress definition is given by the effective pressure P_e (Biot 1955; Christensen and Wang 1985), defined as

$$P_e = P_c - nP_p, \tag{2}$$

and that the differential pressure P_d is only a special case of the effective-stress law when $n = 1$ (i.e. $P_e = P_d$). Until recently, the errors in stress prediction from seismic studies due to this simplification were much lower than other errors. With the improving quality of seismic data, an assumption of $n = 1$ in time-lapse monitoring studies, regardless of the reservoir rock under consideration, can cause significant errors. In such studies, the confining pressure P_c caused by the overburden often remains constant. It is the reservoir fluid pressure P_p, caused by production, which changes. According to equation (2), the change in the effective pressure exerted on the rock frame is

$$\Delta P_e = -n\Delta P_p. \tag{3}$$

Suppose a reservoir rock has $n = 0.5$, then the assumption that $n = 1$ leads to an underestimation of the pore-pressure changes by 100% for a fixed amount of change in velocity and/or an overestimation of the predicted 4D seismic change by 100% for the same pore-pressure change. This might explain the discrepancy between 4D predictions based on $n = 1$ and the actual observations made by Hall *et al*. (2003).

The Biot–Willis coefficient β (Biot and Willis 1957) was originally proposed to describe the ratio of static pore-space deformation to total bulk-volume change. It is given by

$$\beta = 1 - K_{dry}/K_{mineral}, \tag{4}$$

where K_{dry} is the bulk modulus of the dry porous rock and $K_{mineral}$ is the bulk modulus of the constitutive mineral. However, Nur and Byerlee (1971) showed that the effective-stress coefficient of elastic deformation is the Biot–Willis coefficient. Since the Biot–Willis coefficient models the effective-stress coefficient only from dry-rock properties, we speculate that it is the first-order approximation of the effective-stress coefficient.

The Biot–Willis coefficient is a function of porosity as K_{dry} decreases with porosity (Nur *et al*. 1995) for rocks composed of a single kind of mineral. This suggests that the effective-stress coefficient may be a function of porosity, which has been proved by laboratory measurements. Terzaghi (1936) found that the effective-stress coefficient for soils and unconsolidated earth materials (with high porosity) is close to unity. For granite with low porosity, Todd and Simmons (1972) found that the effective-stress coefficient of P-waves is significantly less

than unity. In the same paper, these authors also proposed an experimental formula for the effective-stress coefficient,

$$n_Q = 1 - \frac{[\partial Q/\partial P_p]|_{P_d}}{[\partial Q/\partial P_d]|_{P_p}}, \quad (5)$$

where Q represents any measured rock property.

Even though some trends exist, the data accumulated so far in the literature are too limited to give a complete understanding of the effective-stress coefficient for different lithologies. For example, for Berea sandstone, which is the material on which the most measurements have been made, different researchers obtained substantially different values for the effective-stress coefficient. For the P-wave velocity, Wyllie, Gregory and Gardner (1958) reported $n = 1$, while King (1966) reported n > 1. Christensen and Wang (1985), as well as Prasad and Manghnani (1997), reported values of less than one. These differences might be a direct result of the improving quality of laboratory data.

Here, we present our recent laboratory measurements of the effective-stress coefficient, using equation (5) to compute n. Combining the data and the information available in the literature, we gain deeper insight into how the effective-stress coefficient changes with rock texture and with wave type. We also discuss the implication of these results for 4D seismic feasibility studies, reservoir-pressure inference and pore-pressure prediction.

Table 1 Density, porosity and permeability of samples

	Density (g/cm^3)	Porosity (%)	Permeability (mD)
Unfractured Lyons sandstone	2.475	7.06	0.014
Fractured Lyons sandstone	2.468	7.61	0.016

DESCRIPTION OF SAMPLES

Equation (4) implies that β should decrease with increasing K_{dry}. In other words, the effective stress coefficient should be smaller for stiffer rocks, and low-porosity rocks should deviate most from the assumption of $n = 1$ (Hall *et al*. 2003). Hence, we choose to measure the effective-stress coefficient in low-porosity Lyons sandstone, a Permian aeolian deposit composed of mostly well-sorted quartz grains (90%) with less than 3% of clay. Also, to test the effect on n of changes in K_{dry} without change in porosity, we measured both the original and the microfractured samples. The fractured sample is generated from the original Lyons sandstone using a thermal expansion method. The original Lyons sandstone was put in an oven, and the temperature was gradually increased to 600 °C over a period of three hours and then decreased to room temperature over two hours. Due to the small proportion of clay minerals present in the sample, no significant chemical alteration is introduced by the thermal expansion method. Cylindrical specimens, 6.35 cm (2.5 inches) long and 3.81 cm (1.5 inches) in diameter, were prepared from the original and the fractured Lyons sandstone. The density, porosity and permeability of the samples are listed in Table 1. The porosity and density of the samples were determined by Archimedes' method, and Klinkenberg-corrected permeability was measured using a gas permeameter. The porosity and permeability of the fractured Lyons sandstone are not appreciably different from those of the original Lyons sandstone. Scanning electronic microscopic images (Fig. 1), however, show significant changes in the microstructure of the fractured sample. The original Lyons sandstone is composed of rounded grains with a grain size of about 0.2 mm and is well cemented. The grains themselves do not show microcracks, and grain boundaries are not obvious. The fractured Lyons sandstone, in contrast, shows numerous microcracks along the grain boundaries. The P-wave velocity

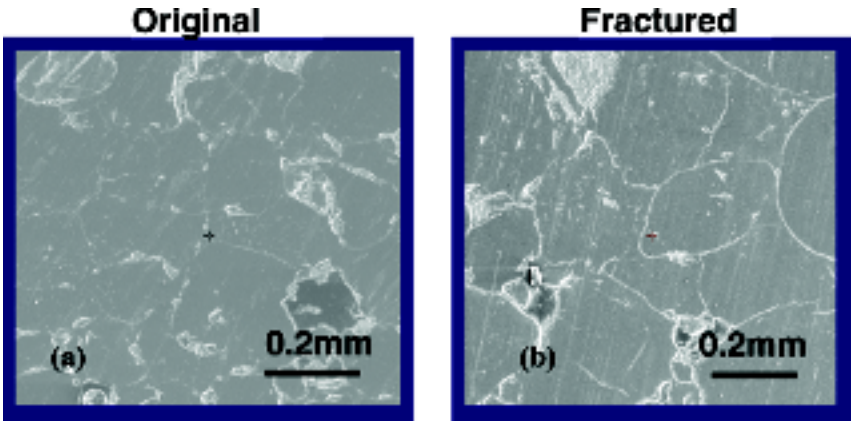

Figure 1 Scanning electronic microscope images of quartz grains and microcracks in (a) the original Lyons sandstone and (b) the fractured Lyons sandstone. Note that the microcracks are easily seen around the grains in the fractured sample.

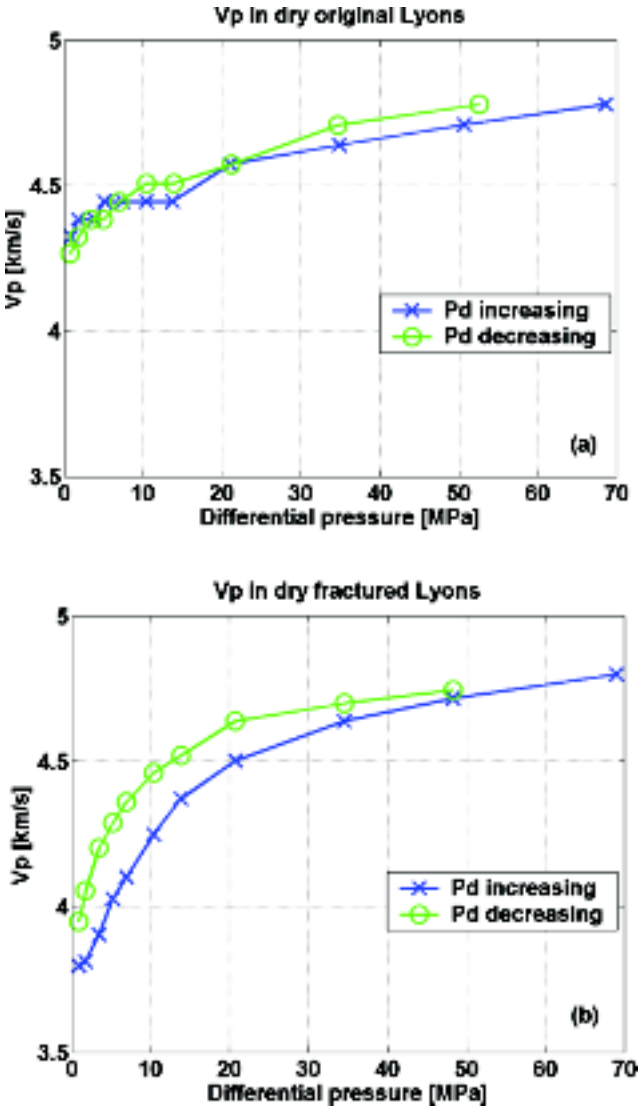

Figure 2 Measurements of P-wave velocity in dry samples. Note that the velocity variation is larger for the fractured Lyons sandstone (b) than for the original Lyons sandstone (a), which is a strong indication of the presence of microcracks in the fractured sample.

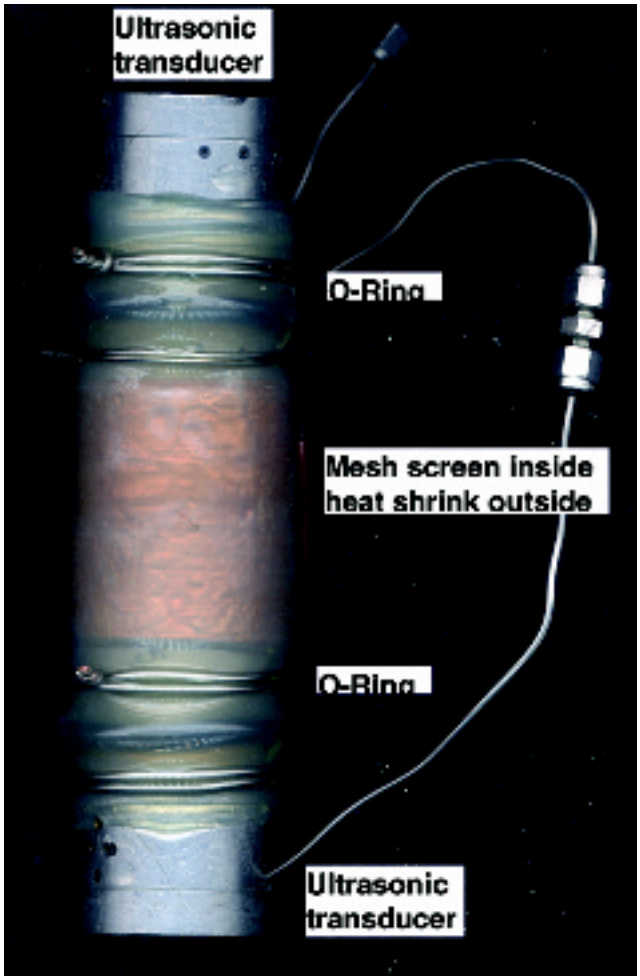

Figure 3 A prepared sample. The sample is wrapped by screen mesh, O-rings and a thick heat-shrink tube.

measurements on dry samples also give a strong indication of the presence of the fractures (Fig. 2). These differences in microstructures will play a role in the observed effective-stress coefficient in both samples.

EXPERIMENTAL SET-UP AND DATA COLLECTION

We measured compressional- and shear-wave velocities in each sample at ultrasonic frequencies (500 KHz) using the pulse transmission technique (Birch 1960). The experimental set-up consists of a hydraulic confining pressure vessel, a pore-pressure controller, a digital oscilloscope, a pulse generator and two ultrasonic transducers attached at the top and bottom of the sample. The core plugs are wrapped in a screen mesh, O-rings and a thick heat-shrink tube (Fig. 3). The screen mesh facilitates fluid passage around the sample. The O-rings and the heat-shrink tube are used to prevent the invasion of hydraulic oil into the sample. Ultrasonic waves passing through the sample are recorded with a sampling interval of 4 ns. Since hand-picking the onset of waves is prone to error, we recorded the waveform and used a cross-correlation technique to measure traveltimes. Velocity is computed as the quotient of length of the sample and the traveltime. The cross-correlation technique gives the velocity measurement with an accuracy of

± 0.2%, which is significantly higher than the accuracy of the hand-picking method (±1%).

For each sample, velocities are measured at different pressures in dry and in butane-and brine-saturated conditions. The sequence of pressure changes is as follows: the confining pressure increases from 14 MPa (2000 psi) to 69 MPa (10000 psi) in increments of 14 MPa (2000 psi), and under each confining pressure, the pore pressure changes from 7 MPa (1000 psi) less than the confining pressure to 7 MPa (1000 psi). Between each measurement, at least half an hour is allowed for equalization of pore pressure in the sample.

The accuracy of our measurements depends on four components: confining pressure, pore pressure, sample length and the traveltime across the sample. The accuracy of the pressure gauges is known to be ±0.5% and the length is within ±0.13% of a centimetre. Since equation (5) involves the derivative of velocity versus pressure, the accuracy of the relative velocity change from one pressure regime to another is more important than that of the absolute velocity. The precision of the relative velocity changes measured by our cross-correlation algorithm is ±0.2%.

DATA PROCESSING

The experimental equation (equation 5) has been used extensively in the literature to compute the effective-stress coefficient (Todd and Simmons 1972; Christensen and Wang 1985; Prasad and Manghnani 1997). Here, we also use this equation to calculate the effective-stress coefficient for the bulk and shear moduli of the rock frame. The bulk and shear moduli of the rock–fluid system (K_{sat} and G_{sat}) can be obtained from the measurements of P-wave and S-wave velocities and density ρ. The density ρ of the rock–fluid system is

$$\rho = \rho_{dry} + \phi\rho_{fl}, \tag{6}$$

where ϕ is the porosity, ρ_{dry} is the density of the dry sample and ρ_{fl} is the density of the fluid saturant. The pressure dependence of ρ_{fl} and of the fluid modulus K_{fl} are computed using the results of Batzle and Wang (1992).

Since we wish to examine the following effects on n:

1 cracks or pore compliance,
2 different saturating fluids,
3 P- and S-wave types,

we need to prepare the measured data in such a way that each effect is isolated. The variation of K_{sat} with pressure results partly from changes in fluid compressibility and partly from changes in the stiffness of the rock frame. To obtain only the changes in the stiffness of the rock frame, we remove the influence of fluid compressibility using Gassmann's equation (Gassmann 1951; in Mavko *et al*. 1998),

$$\frac{K_{norm}}{K_m - K_{norm}} - \frac{K_{fl1}}{\phi\,(K_m - K_{fl1})} = \frac{K_{sat}}{K_m - K_{sat}} - \frac{K_{fl2}}{\phi\,(K_m - K_{fl2})}, \tag{7}$$

where K_{norm} is the normalized bulk modulus of the rock frame, K_{fl1} is the bulk modulus under the normalized condition (the normalized condition is chosen as brine saturation at the lowest measured pore pressure of 7 MPa), K_{fl2} is the fluid modulus at the condition where K_{sat} is measured, and K_m is the bulk modulus of the constitutive mineral.

Strictly speaking, Gassmann's equation cannot entirely eliminate fluid effects in ultrasonic experiments due to the presence of local flow mechanisms, such as squirt flow in the high-frequency regime. The influence of Gassmann's correction is, however, consistent for each pressure condition, and therefore, is expected to have little effect on the effective-stress coefficient which is a function of relative changes in moduli (equation 5).

According to Gassmann's equation, fluid saturation does not change the shear moduli of the rock frame, and therefore

$$G_{norm} = G_{sat}. \tag{8}$$

A graphical interpretation of equation (5) is shown schematically in Fig. 4. To compute the effective-stress coefficient, the

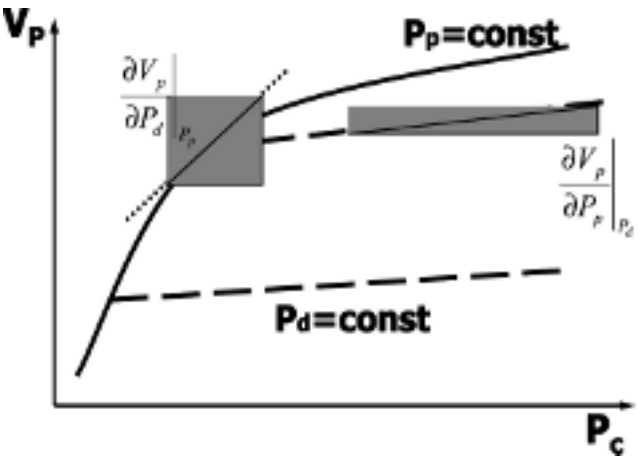

Figure 4 Schematic showing how to compute the numerator and the denominator in the experimental equation of Todd and Simmons (1972) for the effective-stress coefficient(equation 5). The numerator is calculated from the slope of the V_p–P_c curve at constant P_d (V_p could be replaced with any rock property), and the denominator is calculated from the slope of the tangent of V_p–P_c at constant P_p.

numerator in equation (5) is evaluated at constant P_d and the denominator at constant P_p. Therefore, we plot moduli versus confining pressure at constant differential pressure, and at constant pore pressure. At constant P_d, the moduli change linearly with P_c and the slope gives the numerator in equation (5). At a constant P_p, the moduli change with P_d in a logarithmic fashion; hence the tangent is computed to give the denominator in equation (5).

Figure 5 shows an example of the raw data that are measured for a butane-saturated sample. The moduli are plotted as a function of P_c at constant P_d and P_p. The calculated effective-stress coefficients for the normalized bulk and shear moduli of both samples are shown in Fig. 6.

RESULTS

The measured effective-stress coefficients show some distinctive characteristics (Fig. 6). In the following, we list some of the characteristics observed and discuss their possible implications in time-lapse practice in the Discussion section.

1 The effective-stress coefficient n decreases with differential pressure P_d. For instance, n for the bulk moduli of the fractured Lyons is about unity at $P_d = 7$ MPa (1000 psi) and reduces to 0.3 at $P_d = 34$ MPa (5000 psi). This phenomenon is also observed by other laboratory measurements (Todd and Simmons 1972; Hornby 1996; Prasad and Manghnani 1997) and is consistent with the theoretical results of Gangi and Carlson (1996) and Furre (2002).

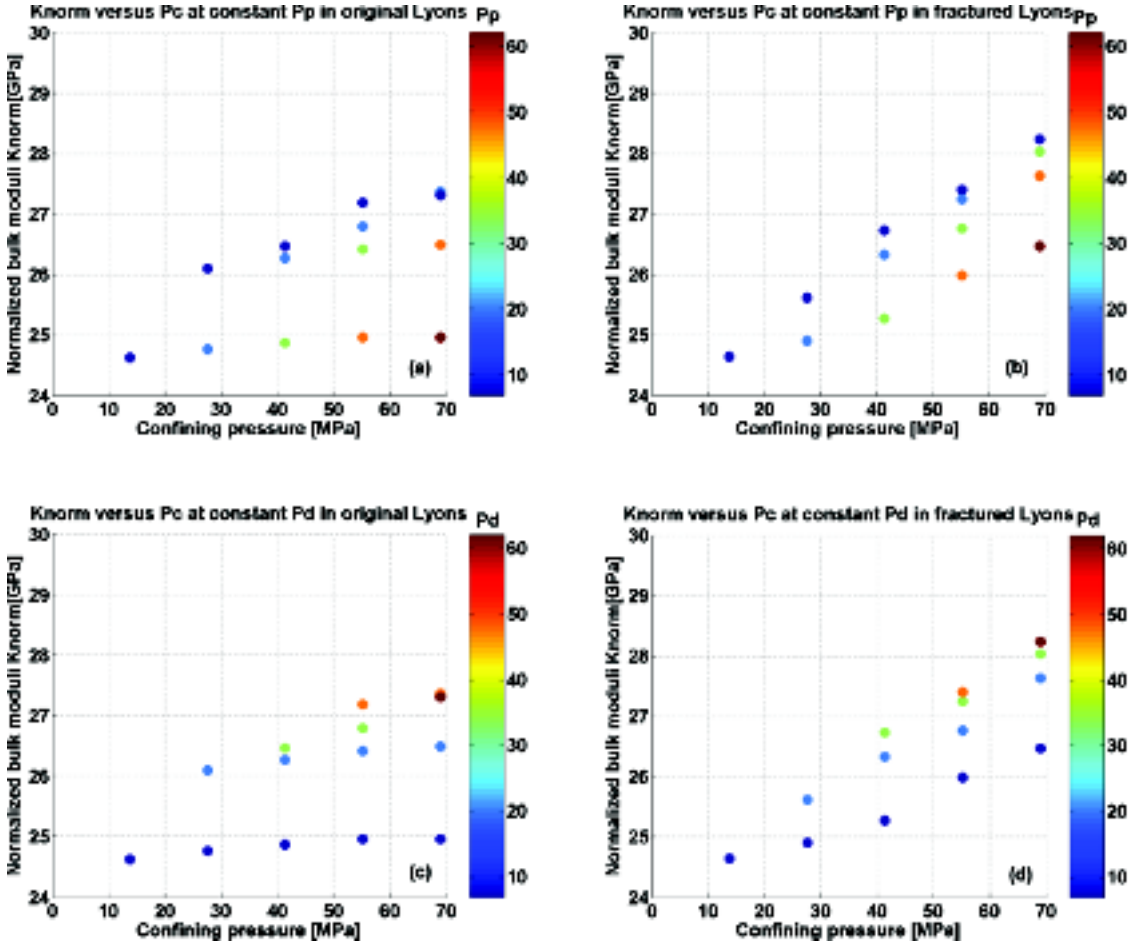

Figure 5 Measured bulk moduli for the original (left) and the fractured (right) Lyons sandstone versus confining pressure. The rock sample is saturated with butane. Colours indicate the pore pressure (top panel) and the differential pressure (bottom panel). The plots at the top are used to compute the denominator in equation (5) and the plots at the bottom are used to compute the numerator in equation (5).

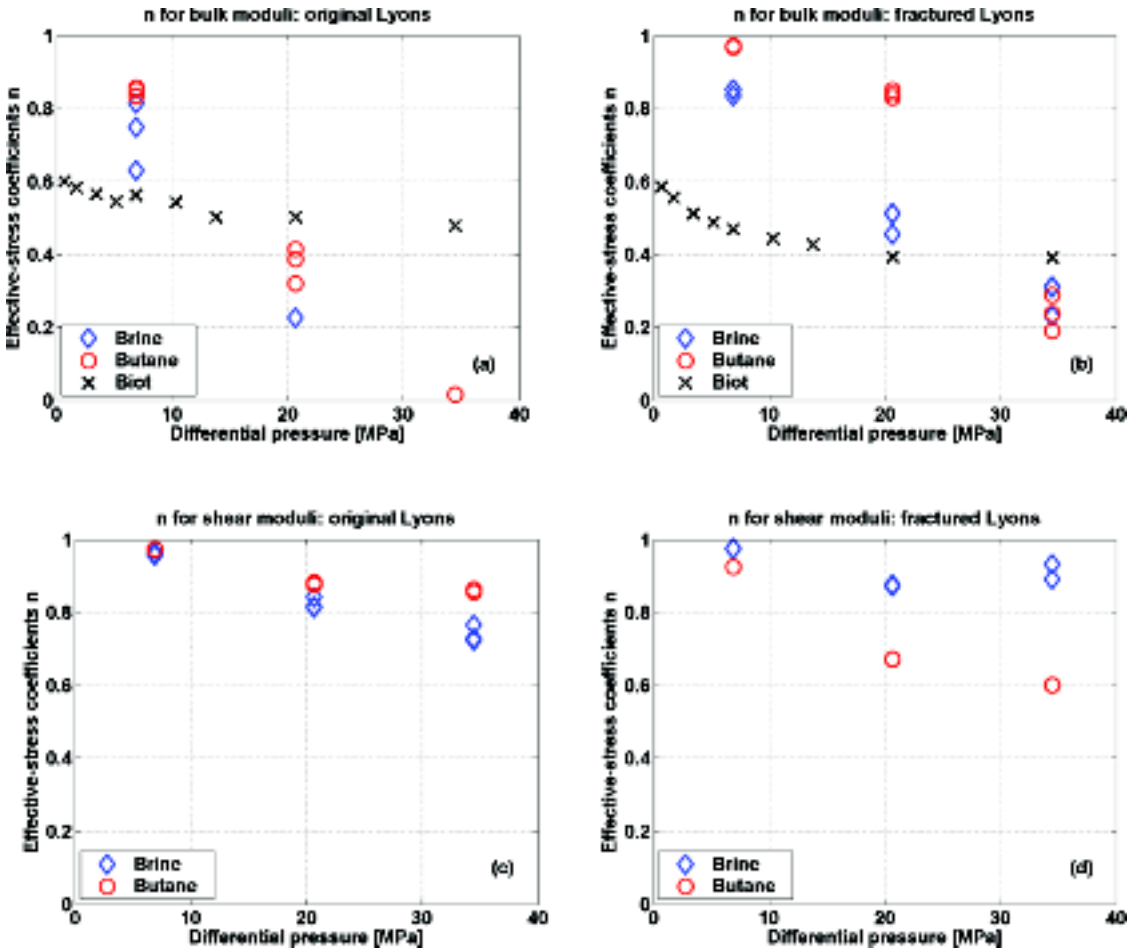

Figure 6 Effective-stress coefficients for the original (left) and the fractured (right) Lyons sandstone as a function of differential pressure and pore fluid (brine and butane). In (a) and (b), the effective-stress coefficients are for the normalized bulk moduli. The Biot–Willis coefficients are also shown for comparison. (c) and (d) show the effective-stress coefficients for the shear moduli. Note that n can be significantly different from unity and it decreases with the differential pressure. See the main text (Results and Discussion) for a further description of n and its implications.

2 Compared with bulk moduli, the effective-stress coefficient for shear moduli is closer to unity at the same P_d. This phenomenon indicates that shear-wave velocities are more sensitive to pore-pressure changes than are compressional-wave velocities. This observation agrees with laboratory measurements (Hornby 1996; Christensen and Wang 1985) and the theoretical results of Nur and Byerlee (1971) and Furre (2002).

3 While the Biot–Willis coefficient predicts that $n < 1$, it fails to predict that n changes with pressure. As shown in Figs 6(a.b), the Biot–Willis coefficient is smaller than the measured effective-stress coefficient at low differential pressure (7 MPa), whereas at high differential pressure (35 MPa), the Biot–Willis coefficient is larger than the effective-stress coefficient. Comparison of the Biot–Willis and the effective-stress coefficients (Figs 6a.b) proves that the Biot–Willis coefficient is the first-order approximation to the effective-stress coefficient.

4 A comparison between Fig. 6(a) and Fig. 6(b) shows that n of the bulk moduli for the fractured sample is larger than that for the original sample under the same pressure conditions. This suggests that the presence of microcracks increases n of the bulk moduli and therefore the influence of the pore pressure on compressional-wave velocities.

5 In Fig. 6(b), each of the three effective-stress coefficients at a fixed P_d corresponds to a different pore pressure. The effective-stress coefficients appear to be independent of pore pressure at a fixed P_d.

By repeating experiments under the same P_d (under different P_c and P_p pairs) and using both butane and brine, we intended to test the statistical significance of the n measurements and

whether the type of pore fluid influences the stress sensitivity of the rock. Figure 6 shows that n is statistically significant; for example, at $P_d = 35$ MPa (5000 psi) in Fig. 6(b), the six values of n range from 0.2 to 0.36. Figure 6 also reveals that even though the values of n for both butane and brine decrease with P_d in a similar manner, they differ at a fixed P_d. Thus, it appears that the fluid type also needs to be considered when evaluating the effective-stress conditions in rocks. Further studies will reveal the systematic nature of this observation.

DISCUSSION

The observations presented here have profound implications for time-lapse and pore-pressure inversion studies in low-porosity sandstones. Our observation that the effective-stress coefficient of bulk moduli decreases with differential pressure is in agreement with the theoretical work of Gangi and Carlson (1996) and Furre (2002), and the experimental work of Todd and Simmons (1972), Christensen and Wang (1985), Hornby (1996) and Prasad and Manghnani (1997). Using spherical packing theory, Furre (2002) showed that, as the differential pressure increases, the contact area between spherical grains flattens and the influence of changes in pore pressure on bulk moduli decreases. One implication of n decreasing with P_d in time-lapse practice is that for deep reservoirs under high P_d conditions, assuming n to be unity may result in very large errors in relating P_p with velocity. If a reservoir composed of fractured Lyons sandstone is at $P_d = 34$ MPa (5000 psi), ignoring the fact that n is about 0.3 instead of unity leads to two errors. On the one hand, for a fixed change in P_p it leads to an overestimate of changes in bulk moduli by a factor of three in feasibility studies; on the other hand, for a fixed observed change in bulk moduli, it results in an underestimate of the change in P_p by about 230%.

Comparing the unfractured with the fractured Lyons sandstone, we observed that the effective-stress coefficients of bulk moduli are larger for the latter, which suggests that the presence of microcracks increases the sensitivity of bulk moduli to pore pressure. This observation is consistent with the findings of Prasad and Manghnani (1997), where the effective-stress coefficient of microcrack-rich Berea sandstone is larger than that of well-cemented Michigan sandstone. In a tight gas–sand reservoir, fractures are often induced to enhance permeability and thus production. The presence of fractures may increase the sensitivity of P-wave velocities to pore-pressure changes, and therefore increase the potential for monitoring changes in pore pressure.

Our measurements on Lyons sandstone show that the effective-stress coefficient for the shear modulus is also less than unity, but larger than that for the bulk modulus. This observation seemingly conflicts with the reports of Christensen and Wang (1985) and Hornby 1996), in which the effective-stress coefficient of the shear wave is larger than unity for Berea sandstone. A conceptual model proposed by Christensen and Wang (1985) might explain the seeming discrepancy. The pore pressure can have a different influence on different components of the rock frame, depending on where in the rock framework the components are situated. For example, mineral linings in pore space are more influenced by pore pressure than are minerals that are an integral part of the rock frame. Since the Berea sandstone contains some clay linings, the pore pressure has more influence on the shear-wave velocity in the Berea sandstone than in the Lyons sandstone, where 98% of the rock is composed of pure quartz grains. Since shear-wave velocity is less sensitive to saturation changes but more sensitive to pore-pressure changes, it can help to distinguish pore-pressure change from saturation change.

Effective-stress measurements are sparse for shales. Since overpressure is usually observed in shale or mudstone, it is not warranted to extrapolate our measurements on sandstone directly to such pore-pressure predictions. If, however, similar phenomena of effective-stress coefficient exist in mudstone (Hornby 1996; Ebrom *et al*. 2004), the accuracy of pore-pressure prediction can be improved by taking the effective-stress coefficient into account (Carcione *et al*. 2003).

ACKNOWLEDGEMENTS

We are indebted to the sponsors of the 'FLUIDS – DHI' consortium and the Center for Wave Phenomena. Stimulating discussions with Manika Prasad helped us understand the subject better. The first author is also grateful to Hans Ecke who taught her how to manipulate the ultrasonic equipment at the Center of Rock Abuse.

REFERENCES

Batzle M. and Wang Z. 1992. Seismic properties of pore fluids. *Geophysics* **57**, 1396–1408.

Biot M.A. 1955. Theory of propagation of elastic waves in a fluid-saturated porous solid. II. Higher frequency range. *Journal of the Acoustical Society America* **28**, 179–191.

Biot M.A. and Willis D.G. 1957. The elastic coefficients of the theory of consolidation. *Journal of Applied Mechanics* **24**, 594–601.

Birch F. 1960. The velocity of compressional waves in rocks to 10 kilobars, Part 1. *Journal of Geophysical Research* **65**, 1083–1102.

Carcione J.M., Helle H.B., Pham N.H. and Toverud T. 2003. Pore pressure estimation in reservoir rocks from seismic reflection data. *Geophysics* **68**, 1569–1579.

Christensen N.I. and Wang H.F. 1985. The influence of pore pressure and confining pressure on dynamic elastic properties of Berea Sandstone. *Geophysics* **50**, 207–213.

Ebrom D., Heppard P., Thomsen L., Mueller M., Harrold T., Phillips L. and Watson P. 2004. Effective stress and minimum velocity trends. 74th SEG Meeting, Denver, USA, Expanded Abstracts, 1615–1618.

Furre A. 2002. The effective stress coefficient for wave velocities in saturated grain packs. 64th EAGE Conference, Florence, Italy, Extended Abstracts, P093.

Gangi A.F. and Carlson R.L. 1996. An asperity-deformation model for effective pressure. *Tectonophysics* **256**, 241–251.

Gassmann F. 1951. Elasticity of porous media. *Vierteljahresschrift der Naturforschenden Gesselschaft* **96**, 1–23 (in German).

Hall S.A., MacBeth C., Stammeijer J. and Ormerod M. 2003. Time-lapse seismic analysis of pressure depletion in the Southern Gas Basin. 73rd SEG Meeting, Dallas, USA, Expanded Abstracts, 1374–1377.

Hornby B. 1996. An experimental investigation of effective stress principles for sedimentary rocks. 66th SEG Meeting, Denver, USA, Expanded Abstracts, 1707–1710.

King M.S. 1966. Wave velocities in rocks as a function of overburden pressure and pore fluid saturants. *Geophysics* **31**, 56–73.

Landrø M., Veire H.H., Duffaut K. and Najar N. 2003. Discrimination between pressure and fluid saturation changes from marine multicomponent time-lapse seismic data. *Geophysics* **68**, 1592–1599.

MacBeth C., Stammeijer J. and Ormerod M. 2006. Seismic monitoring of pressure depletion evaluated for a UKCS gas reservoir. *Geophysical Prospecting* **52**, 29–47.

Mavko G., Mukerji T. and Dvorkin J. 1998. The Rock Physics Handbook: *Tools for Seismic Analysis in Porous Media*. Cambridge University Press.

Nur A. and Byerlee J.D. 1971. An exact effective stress law for elastic deformation of rocks with fluids. *Journal of Geophysical Research* **76**, 6414–6419.

Nur A.M., Mavko G., Dvorkin J. and Gal D. 1995. Critical porosity: the key to relating physical properties to porosity in rocks. 65th SEG Meeting, Houston, USA, Expanded Abstracts, 878–881.

Prasad M. and Manghnani M. 1997. Effects of pore and differential pressure on compression wave velocity and quality factor in Berea and Michigan sandstones. *Geophysics* **62**, 1163–1176.

Terzaghi K. 1936. Relation between soil mechanics and foundation engineering: Presidential address. Proceedings of 1st International Conference on Soil Mechanics and Foundation Engineering. *Boston* **3**, 13–18.

Todd T. and Simmons G. 1972. Effect of pore pressure on the velocity of compression waves in low-porosity rocks. *Journal of Geophysical Research* **77**, 3731–3743.

Wyllie M.R.J., Gregory A.R. and Gardner G.H.F. 1958. An experimental investigation of factors affecting elastic wave velocities in porous media. *Geophysics* **23**, 459–493.